

## About NICADD Extruded Scintillating Strips

A. Dyshkant, D. Beznosko, G. Blazey, D. Chakraborty, K. Francis, D. Kubik, J. G. Lima,  
V. Rykalin, V. Zutshi  
Department of Physics, Northern Illinois University, DeKalb, IL 60115

E. Baldina, A. Bross, P. Deering, T. Nebel, A. Pla-Dalmau, J. Schellpfeffer, C. Serritella,  
J. Zimmerman  
Fermilab, Batavia, IL 60510

### Abstract

The results of control measurements of extruded scintillating strip responses to a radioactive source Sr-90 are provided, and details of strip choice, preparation, and method of measurement are included. About four hundred one meter long extruded scintillating strips were measured at four different points. These results were essential for prototyping a tail catcher and muon tracker for a future international electron positron linear collider detector.

### Introduction

In a few years, the LHC opens a new fertile field in TeV-scale high-energy physics. The future electron-positron international linear collider (ILC) will be the next major TeV-scale step that will deliver a higher precision and a deeper understanding of new physics processes. To take full advantage of the physics potential of the future electron-positron linear collider, the detector (ILCD) in Fig.1 [1] should have unprecedented performance in each of its components, or parameters.

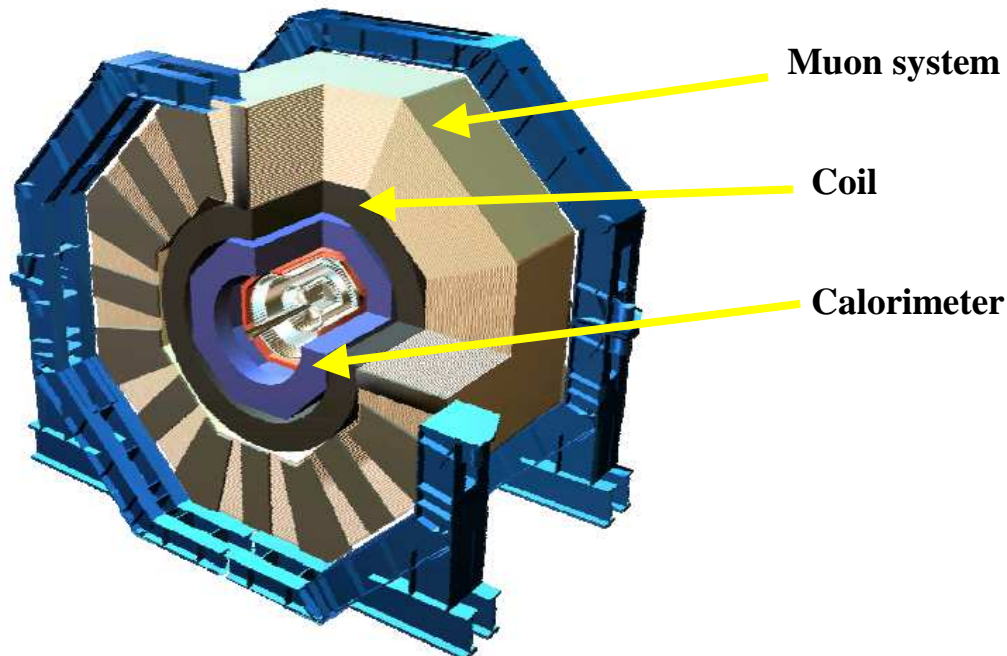


Fig. 1. General view of a future Si linear collider detector [1].

For example, the ability to distinguish W and Z bosons by their decay into two jets will require a jet energy resolution of  $\sigma/E \sim 30\%/\sqrt{E}$ . Particle flow algorithms (PFA) appear to be the most promising way to achieve such performance in jet energy measurements. To fully exploit PFA, the calorimeter should be highly segmented in transverse and longitudinal directions, and the ILCD itself should be optimized for the application of PFA.

Hermeticity and resolution constraints require the calorimeter to be placed inside a superconductive coil. Because of this constraint, the hadron calorimeter will be compact and limited to a depth of approximately 1 m. The relatively thin hadron calorimeter requires additional “calorimetric sampling” behind the superconductive coil to estimate and correct for the hadronic leakage. Such sampling also offers excellent muon tracking.

Consequently, Northern Illinois Center for Accelerator and Detector Development (NICADD) has undertaken the construction of a combined hadronic tail-catcher and muon tracker (TCMT) prototype. NICADD simulations of the electromagnetic and hadronic calorimeters with TCMT using Geant4 indicate that energy resolution of charged pions ( $\sigma/E$ ) can be 30% or better in the energy region 20-50 GeV only when the energy from the tail-catcher is included. A design for the TCMT prototype consists of 16 steel absorber layers and sixteen active medium cassettes with dimensions of about 1m x 1m. NICADD proposed using extruded scintillating strips as the active medium for the TCMT. Each cassette has ten extruded scintillating strips with thickness of 5 mm, width of 10 cm, and length of approximately 1 m.

NICADD will explore TCMT performance with CALICE beam test [2]. An ILCD proposal for a CALICE test beam program at Fermilab includes a wide variety of combined tests with TCMT. The test will provide the first experience in ILCD prototyping, muon ID and reconstruction, parameterization of the superconducting coil impact on energy resolution, and enable development of algorithms for restoring the energy resolution within the particle flow framework.

In this note, the results of control measurements of response to a radioactive source for the strips, which were extruded in two production runs, are provided. In addition, the details of strip choice, preparations, and method of measurements are included. These measurements form a key basis for the quality control of strips to be used for the TCMT prototype. Moreover, the experience gained will be useful for a wide variety of researchers, who may want to use extruded scintillator for their experiments.

### **Strip choice**

For the TCMT prototype, the MINOS [3] scintillating strips meet specifications. Because those strips are not available, the 5 mm thick and 10 cm wide NICADD extruded scintillating strips [4] were a possible choice. Because 10 cm strip is too wide for the basic TCMT design (can not provide sufficient segmentation), each strip should be cut in half, or a separation groove must be introduced. The choice was governed by the following considerations. First, for the estimation of an available amount of light, a 1 m long strip with a co-extruded hole was tested with cosmic rays. A 1.2 mm outer diameter Kuraray [5] Y-11 multicladd S-type WLS fiber was glued inside the hole using EJ-500 [6] optical glue. With a Hamamatsu [7] R-580 PMT, the strip provided 14.4 photoelectrons (PE). Second, because the optical cement lost transmission even at a low radiation dose,

strips with a machined “key” shape groove (Fig. 2) for the WLS fiber were also tested. The groove had the following dimensions: an inner diameter of 0.053”, a width of neck 0.040”, and it was done for the four different depths (h): 0.063”, 0.078”, 0.117”, and 0.156”. The respective PE yields were 12.3, 13.9, 14.3, and 13.3 PE. Finally, a strip with a small co-extruded hole was tested in the same way. The inner diameter of the co-extruded hole was about the outer diameter of the WLS fiber (1.2mm). The extruded strip with the small co-extruded hole and non-glued WLS fiber provided 15.2 PE. Because the mean value of diameter and position of the co-extruded hole can be adjusted during the production run, the NICADD extruded strip with the small co-extruded hole was the final choice for the TCMT.

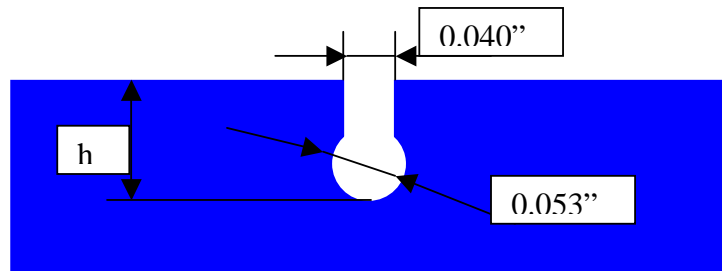


Fig. 2. Groove schematic and dimensions.

### Strip preparation

1.05 m long, 10 cm wide, and 5 mm thick extruded scintillating strips [4] had two co-extruded holes at about 25 mm from the edges, as in Fig.3a). The inner diameter of the co-extruded holes was not less than 1.2 mm. At 50 mm from the strip edge, a 1.01 m long and 0.9 mm wide separation groove was milled through the strip with a computer-controlled machine (THERMWOOD) at Fermilab Lab8.

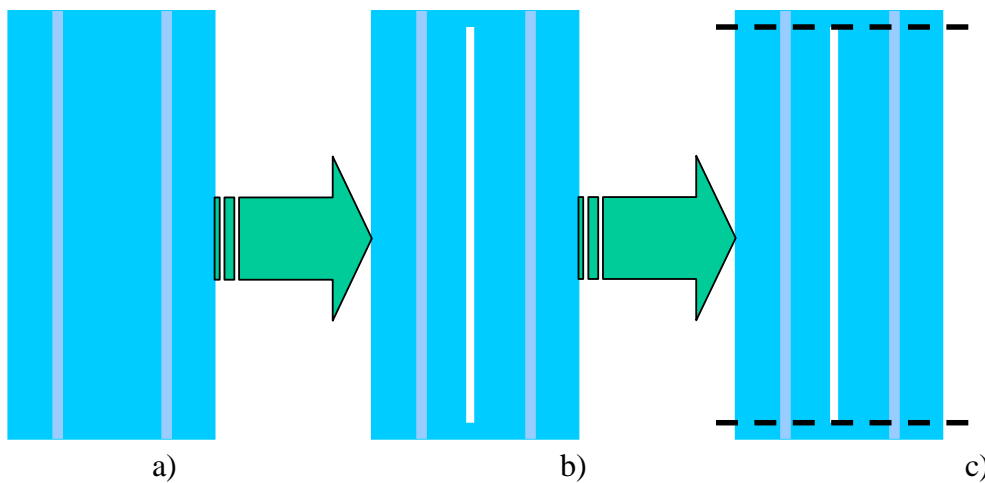


Fig. 3. Strip preparation

The scintillating strips were cleaned after machining and removed from the machine table to a gluing facility. There, using blue tape [8], the separation groove was tightly taped on the top and on the bottom of the strip surfaces and then injected with a white epoxy [9] (an epoxy resin DER332, with 50% of a titanium dioxide and the hardener Jeffamine D230) as shown in Fig.3b. After the epoxy hardened, all tape was removed and the strips were put back on the computer-controlled machine where the ends were cut off to the 1.01 m strip length (Fig.3c). The white epoxy serves as a reflective material, and is also used to reduce crosstalk between created strips and improve their structural rigidity. Step-by-step modifications of the strip are also shown in Fig. 4.

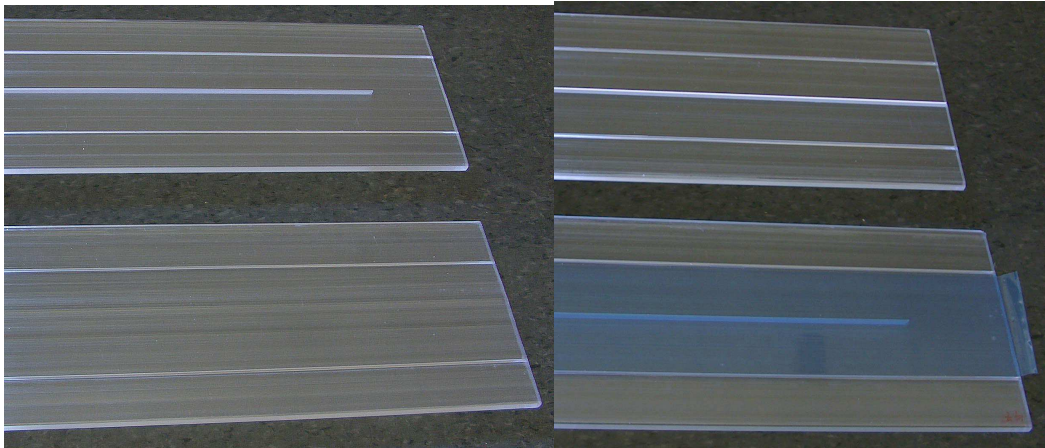


Fig. 4. At left bottom is a strip after extrusion; at left top is the same strip with a machining separation groove; at right bottom is the strip with blue tape; at right top is the trimmed strip with the glued separation groove.

### Strip measurement method

A schematic of the measurement configuration schematic show in Fig.5 consists of two reference cells (RC) [10] and a few WLS fibers permanently connected to a Hamamatsu [7] R580 PMT via an optical crystal [11]. The crystal mixed the light from fibers and reduced non-uniformity of responses across the PMT photocathode to less than 1%. The WLS fibers were Kuraray [5] Y-11, multiclاد, S-type, 1.2 mm outer diameter and 1.15 m length. Their ends were ice polished using a “P3” diamond cutter machine. One fiber end was aluminum mirrored using a magnetron gun sputtering technique [12]. The other end of fiber was glued in a 1.5 mm diameter hole inside a square plastic ferrule (4.3 mm side width and 35 mm length) and then polished together with the ferrule using a “diamond fly” cutting technique. The ferrule helps to orient the polished surface of the fiber at a right angle with respect to the optical crystal, and provide firm connection. It was possible to connect up to sixteen ferrules at the same time to the crystal. The PMT output current was measured with a picoammeter [13], connected to a PC-based data acquisition system.

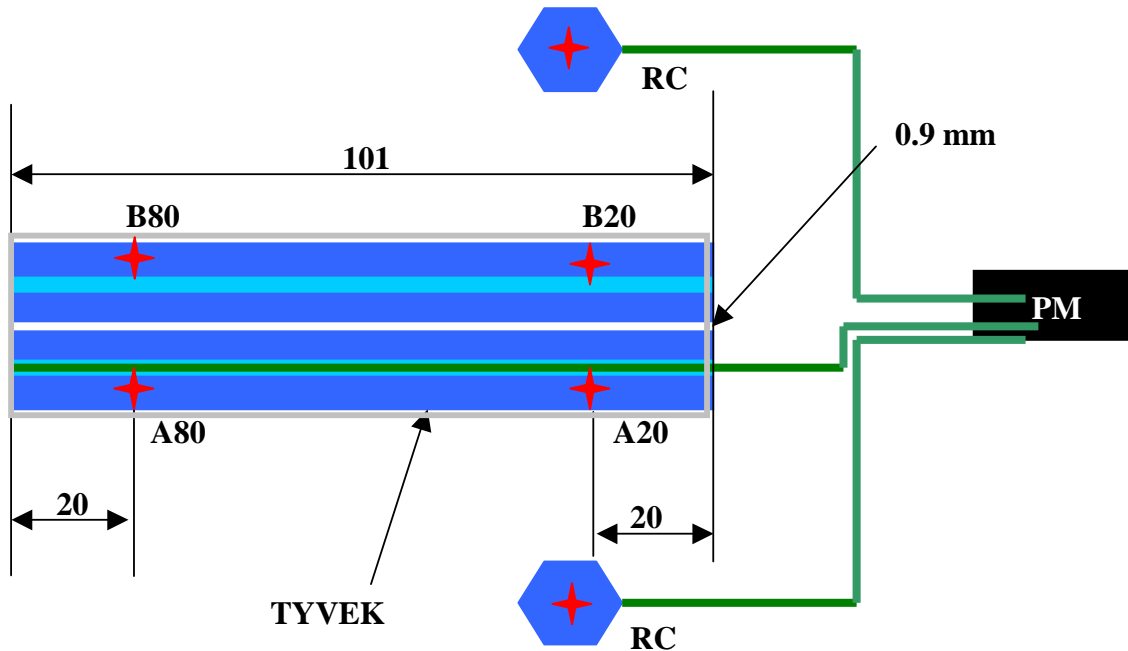


Fig. 5. Schematic of setup used for a strip measurement. (Dimensions are in mm). The letters RC denote the reference cells.

The strips were wrapped in a 1 m long sleeve made from one layer of Tyvek [14]. Same Tyvek sleeve was used for all measurements. The strip ends were neither painted nor wrapped. Because a co-extruded hole has somewhat oval rather than circular shape, and a specific orientation inside a strip, it was possible to define a top and a bottom of the strip, as indicated in Fig. 6a and Fig. 6b. In all cases, the distance from the WLS fiber to the strip bottom was less than the distance from the fiber to the strip top. A 5 mCu Sr-90 radioactive source was positioned on the top surface at 15 mm from the strip edge.

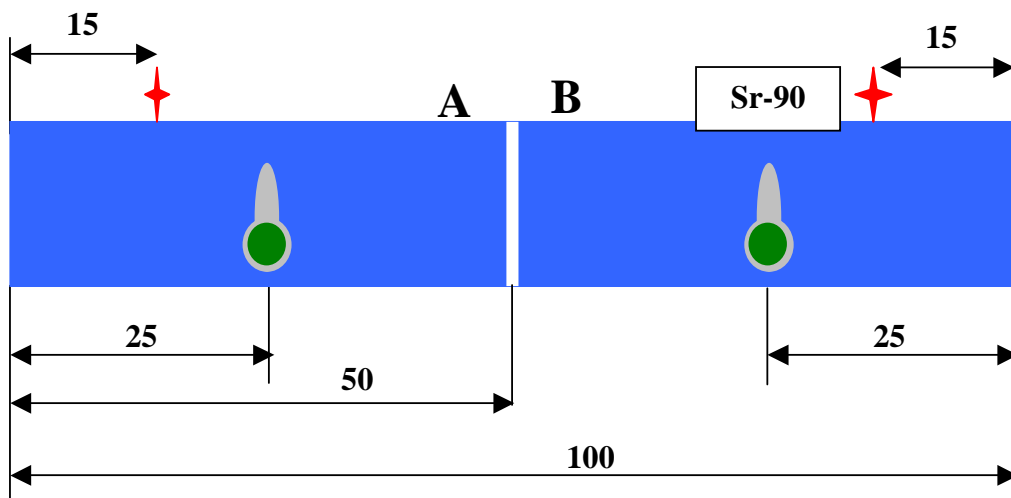


Fig. 6a. A setup schematic used for a strip orientation and a radioactive source positioning. (Dimensions are in mm).



Fig. 6b. Co-extruded hole shapes. At the ends of the strips, positions of the four holes were measured. The average distance from the edge of the strip to the “center” of the hole was 23.5 mm with standard deviation of 0.2 mm.

To ensure reproducibility of the source positioning better than 1 mm, a template was used. The same WLS fiber was used for most of the measurements. Once the strip was placed for measurements and the WLS fiber was inserted into the co-extruded hole, the side of the strip closest to the experimenter was labeled “A” while the furthest one was assigned the label “B”, as indicated in Fig.5. It was a random choice which part of a strip was named A or B.

The major steps in measuring the strip response were:

1. The response of the first reference cell with the radioactive source placed in the center of the cell was measured.
2. The response of the second reference cell with the radioactive source placed in the center of the cell was measured.
3. With the WLS fiber inserted consistently to the end of the co-extruded hole and high voltage on, but without the radioactive source, the dark current was measured for each strip. The maximum value of the dark current was less than 0.5 nA for all measurements.
4. The response of the A-side of a strip with the radioactive source placed at 80 cm from the PMT end was measured (Fig. 5).
5. The response of the A-side of the strip with the radioactive source placed at 20 cm from the PMT end was measured.
6. The response of the B-side of the strip with the radioactive source placed at 80 cm from the PMT end was measured.
7. The response of the B-side of the strip with the radioactive source placed at 20 cm from the PMT end was measured.

Steps 3 to 7 were repeated for the each strip. Each set of measurements was started and finished with steps 1 and 2. If at the end of each set of measurements the reference cell response was similar to the response at the beginning, the strip responses were accepted for further analysis. The

mean value of the reference cell response ratio (finish to start) for 29 consistent measurements was 1.001 with a standard deviation of 0.015. Because this test did not fail, all strip responses were accepted for analysis.

### Results

To estimate possible degradation over time, the responses of a few strips (#77, 78, and 79) were measured at the beginning of tests (09.16.2004), and were measured again after all the strips were tested (10.15.2004). Table I provides the new and the old data, including the date. The average value of ratios of the new responses to the old ones is  $0.961 \pm 0.002$ , which means that the degradation over time is about 4%. Because the NICADD extruded scintillator [15] cannot degrade so fast, it means that the measurement system does. The visual inspection showed that it was the WLS fiber, especially the mirrored end (keep in mind that this fiber was inserted into the co-extruded holes up to eight hundred times). Because of the small degradation of the measuring system over the long time interval, no corrections were applied to the measurements. Fig.7 and Fig.8 show the response of the strip A-side. A few of them have a much lower response at 80 and 20 than average.

Table I. Ratio of responses of several strips (in  $\mu\text{A}$ ) measured at the beginning of the test to measured after the end of measurements of all other strips.

DATE	STRIP #	A80	A20	B80	B20
09.16.04	77	1.507	1.804	1.571	1.795
10.15.04	77	1.445	1.719	1.514	1.738
09.16.04	78	1.500	1.801	1.531	1.798
10.15.04	78	1.437	1.721	1.460	1.740
09.16.04	79	1.530	1.779	1.555	1.751
10.15.04	79	1.458	1.697	1.502	1.709

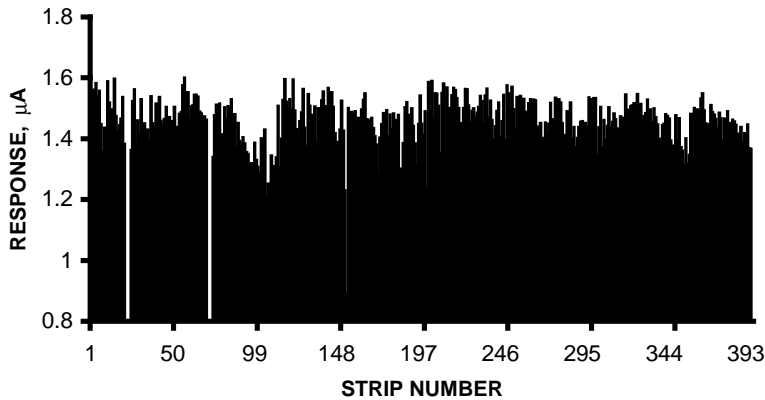


Fig. 7. Strip responses as measured at position A80.

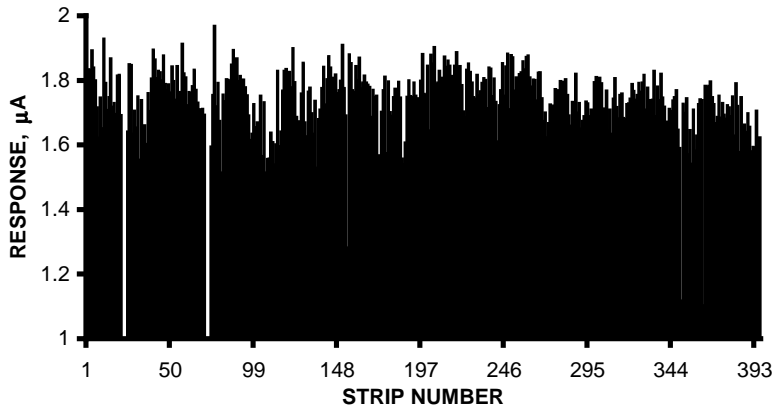


Fig. 8. Strip responses as measured at position A20.

The distribution in Fig.9a and Fig. 9b, which is the ration of the response at A20 to response at A80, is an indication of the uniformity response for all measured strips. Fig. 10 illustrates the same for each strip in a different format; a few of them are far from the average.

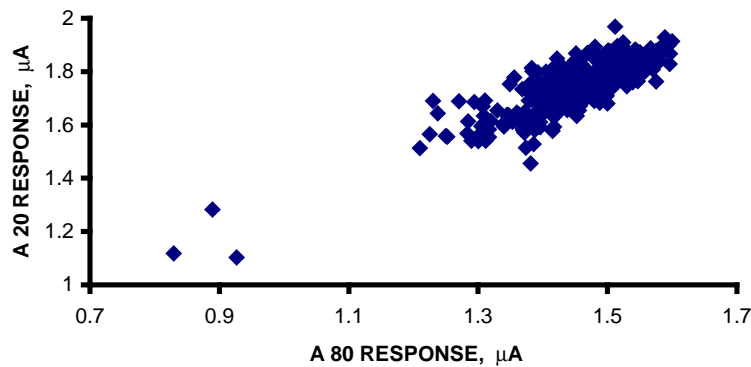


Fig. 9a. A20 response versus A80 (all strips) illustrates the brightness (at 20) and attenuation (at 80) for each strip.

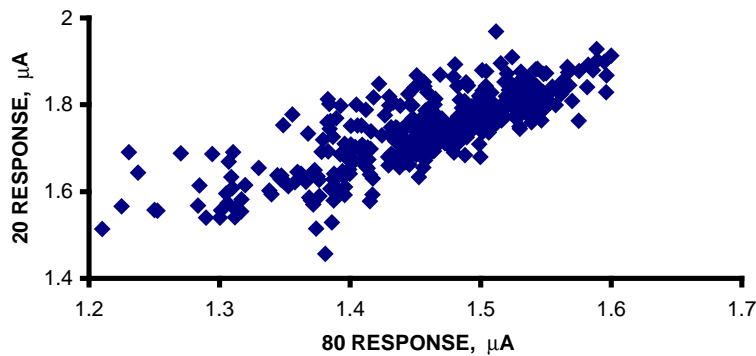


Fig. 9b. A20 versus A80 distribution, as in 9a, but without 3 strips with lower response.

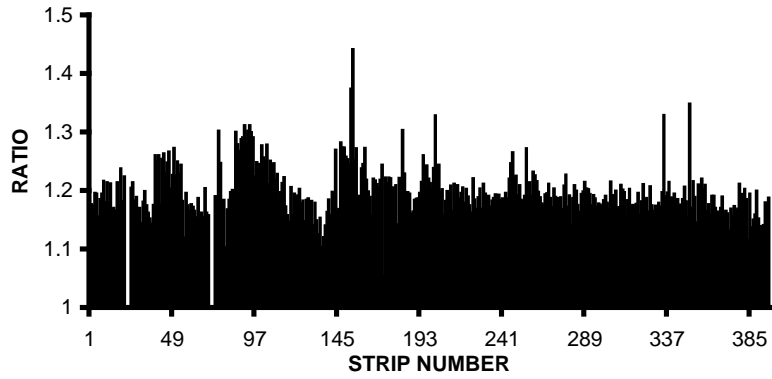


Fig. 10. Ratio A20/A80 versus number of the strips

Figs. 11-14 illustrate the same results for sides B of the strips that are similar to sides A results. The frequency of response for position A80, A20, B80, B20 and their ratios are shown in Table II.

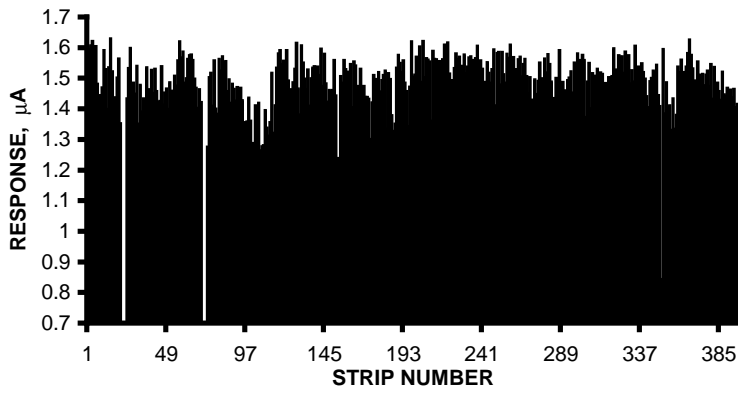


Fig. 11. Strip responses as measured at position B80.

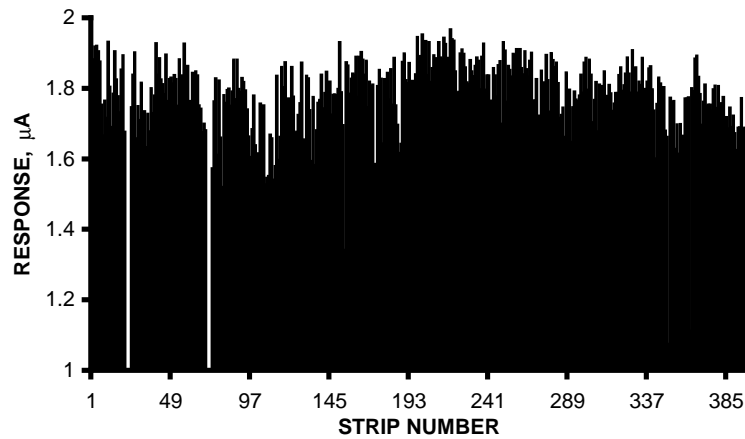


Fig. 12. Strip responses as measured at position B20.

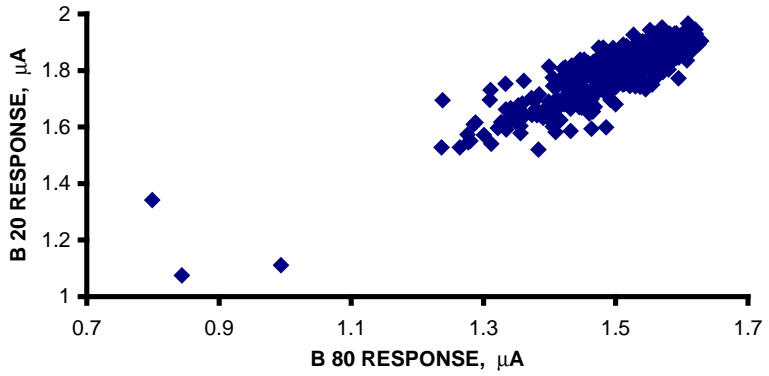


Fig. 13a. B20 response versus B80 response for all strips

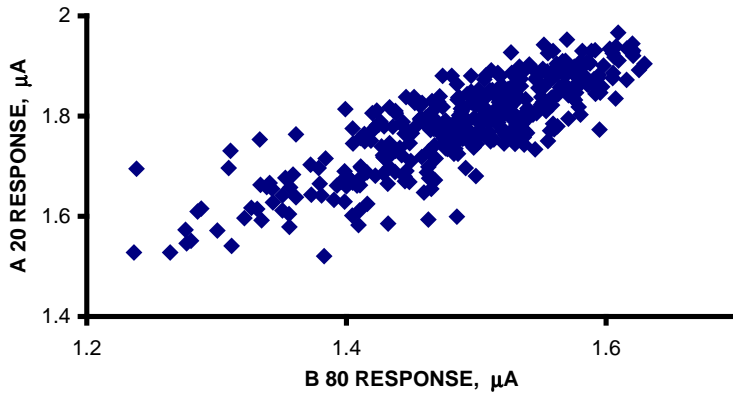


Fig. 13b. A20 response versus B80 response without 3 strips with lower responses

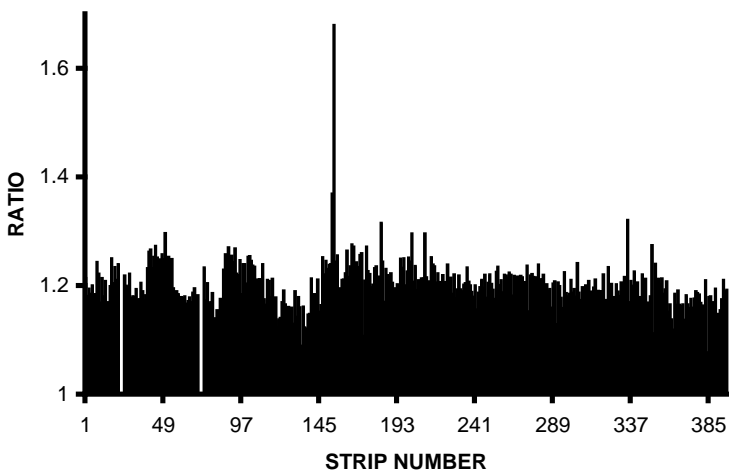


Fig. 14. Ratio B20/B80 versus number of the strips

Table II. Frequency for strip responses (in  $\mu\text{A}$ ) and their ratio

VALUE	RESPONSES ( $\mu\text{A}$ )				RATIO	
	A80	A20	B80	B20	A20/A80	B20/B80
1.00	3	0	3	0	0	0
1.05	0	0	0	0	0	0
1.10	0	0	0	1	1	3
1.15	0	2	0	1	22	29
1.20	0	0	0	0	226	166
1.25	4	0	2	0	99	161
1.30	7	1	6	0	32	27
1.35	21	0	14	1	8	2
1.40	47	0	22	0	1	1
1.45	73	0	59	0	1	0
1.50	116	1	90	0	0	0
1.55	91	6	98	5	0	0
1.60	28	19	79	10	0	0
1.65	0	32	17	17	0	0
1.70	0	47	0	40	0	1
1.75	0	86	0	37	0	0
1.80	0	94	0	94	0	0
1.85	0	70	0	85	0	0
1.90	0	27	0	69	0	0
1.95	0	4	0	28	0	0
2.00	0	1	0	2	0	0

Fig. 15 shows ratio for A80/B80 and A20/B20 for each strip. The frequencies for these ratios are given in Table III. Except for a few strips, the A80/B80 and A20/B20 ratios are highly uniform with about 2% asymmetry (for 382 strips the mean value of A80/B80 ratio is 0.979, minimum is 0.935, maximum is 1.028, and standard deviation is 0.018).

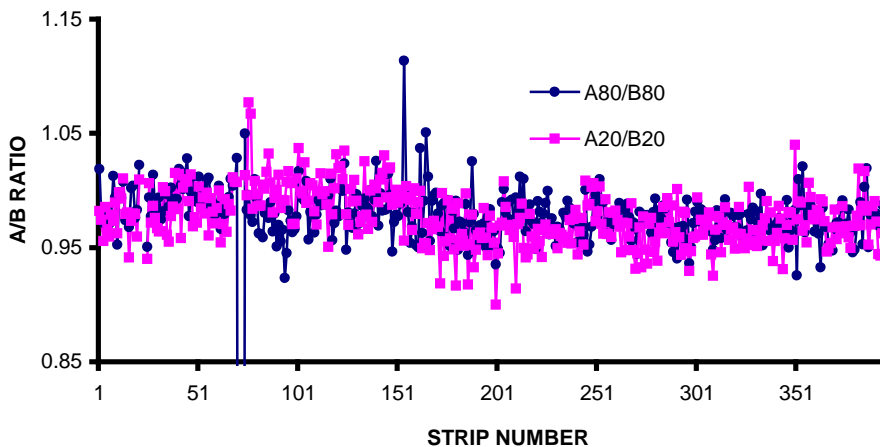


Fig. 15. Asymmetry across the strip. (Strip number not associated with production time.)

In a separate study that consisted of the same strips, sleeve, and the measurement setup, an indication of the sleeve asymmetry of about 3% was detected. The pieces of the blue tape (Fig. 16b), which hold together the edges of the Tyvek in the form of a sleeve (Fig. 16a), create an asymmetry through additional absorption of scintillating light.

Table IV shows number of strips and parameter values, which help recognize “bad” strips. The following cut parameter values were chosen using the frequency Table II:

- A80 or B80 response less than 1.25  $\mu\text{A}$ : selects three strips.
- A20 or B20 response less than 1.50  $\mu\text{A}$ : selects three strips.
- A20/A80 or B20/B80 ratios more than 1.30: selects respectively ten and four strips.

Using those cut parameter values and Fig. 7, 8, 10-12, and 14 the “bad” strip numbers were recognized. “Bad” strips convert into only twelve different strip numbers. It was easy to visually pre-select strips #148, 343, and 356 as bad because those strips had noticeably weaker blue color under ultraviolet (UV) light source than all the other strips.

Table III. Frequency for ratio A80/B80 and A20/B20 (or asymmetry across the strips)

<b>VALUE</b>	<b>A80/B80</b>	<b>A20/B20</b>
<b>0.90</b>	<b>0</b>	<b>1</b>
<b>0.91</b>	<b>0</b>	<b>0</b>
<b>0.92</b>	<b>0</b>	<b>4</b>
<b>0.93</b>	<b>2</b>	<b>2</b>
<b>0.94</b>	<b>3</b>	<b>8</b>
<b>0.95</b>	<b>18</b>	<b>33</b>
<b>0.96</b>	<b>32</b>	<b>51</b>
<b>0.97</b>	<b>70</b>	<b>71</b>
<b>0.98</b>	<b>94</b>	<b>58</b>
<b>0.99</b>	<b>73</b>	<b>55</b>
<b>1.00</b>	<b>51</b>	<b>42</b>
<b>1.01</b>	<b>21</b>	<b>36</b>
<b>1.02</b>	<b>15</b>	<b>18</b>
<b>1.03</b>	<b>7</b>	<b>3</b>
<b>1.04</b>	<b>1</b>	<b>6</b>
<b>1.05</b>	<b>1</b>	<b>0</b>
<b>1.06</b>	<b>1</b>	<b>0</b>
<b>1.07</b>	<b>0</b>	<b>1</b>
<b>1.08</b>	<b>0</b>	<b>1</b>
<b>1.09</b>	<b>0</b>	<b>0</b>
<b>1.10</b>	<b>0</b>	<b>0</b>
<b>1.11</b>	<b>0</b>	<b>0</b>
<b>1.12</b>	<b>1</b>	<b>0</b>

Table IV. Numbers of “bad” strips with cut value parameters listed.

PARAMETER	STRIP NUMBER											
	A80 (<1.25)	356	343				148					
A20 (<1.50)	356	343				148						
B80 (<1.25)	356	343				148						
B20 (<1.50)	356	343				148						
A20/A80 (>1.30)			339	196	177	148	147	89	88	85	80	70
B20/B80 (>1.30)			339	196	177	148	147					



Fig. 16. a) Tyvek sleeve, b) pieces of blue tape (bottom) used in the measurements. The tape caused the A/B asymmetry.

The strips that exhibited lower responses were further investigated to determine the cause of the problem. Since those strips presented a weaker blue color under UV light source than the other strips, a fluorescence test was performed to check the dopant concentrations. A Hitachi [16] F-4500 fluorescence spectrophotometer was used. Several samples (2.5 cm wide) were cut from the strips with both high and low responses. The fluorescence spectra from those samples were compared to the reference-scintillating sample with known dopant concentrations as shown in Fig. 17. The dopants for the strips were 1% PPO (primary) and 0.03% POPOP (secondary). The emission maxima for PPO and POPOP are at approximately 365 nm (peak A) and 420 nm (peak B), respectively. It is known from previous work that the ratio between those two peaks (B/A) needs to be

above 1.2 in order to have a high quality scintillator. The sample from the lower response strip shows a deviation in the dopant concentrations and the B/A ratio of the two peaks is below the threshold. Those strips were likely collected at the end of the extrusion production when the dopant feeder was nearly empty and only traces of PPO were added.

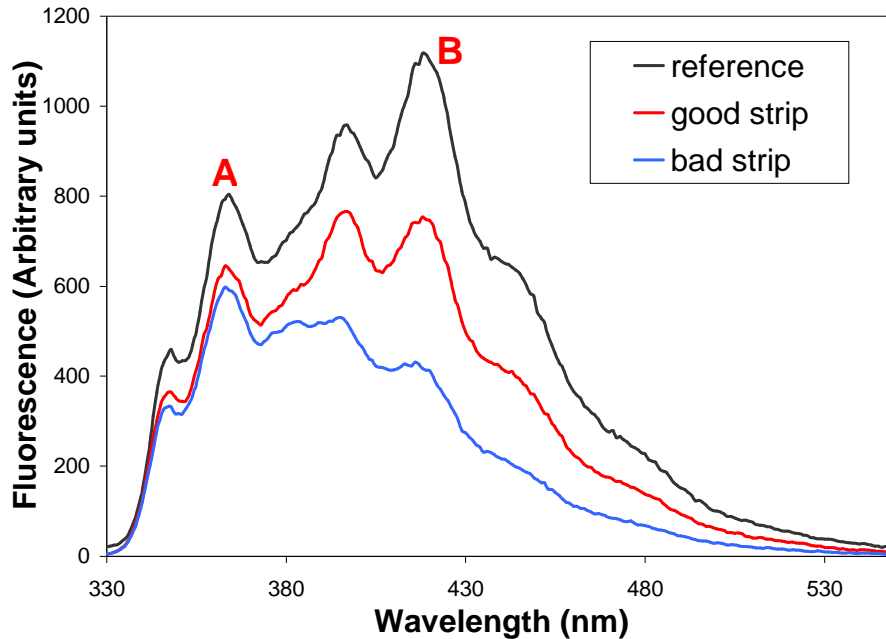


Fig. 17. Fluorescence spectra of three extruded scintillator samples: in black, the reference; in red, from a strip with good response; and in blue, from a strip with lower response.

### Conclusion

The high uniformity of strip responses (brightness, attenuation length and asymmetry) provides evidence that a high quality extrusion-scintillating product is available. Detailed measurements of the extruded strips and analysis of the strip responses readily identify poor quality strips. The total number of “bad” strips is about 3% of two production runs.

### Acknowledgments

The authors would like to thank Daniel Ruggiero and Dave Burk for help; Scott Carlson and Jerry Taccki for excellent mechanical and machining support. This work was supported in part by the U.S. Department of Education grant #P116Z010035, the Department of Energy and the State of Illinois Higher Education Cooperation Act. The work at Fermilab was supported by the U.S. Department of Energy under contract #DE-AC02-76CHO3000

## References

- [1] *ILC Detector Design and R&D*, Harry Weerts, ILC Meeting at Fermilab, October 27, 2004
- [2] *International Linear Collider Calorimeter Test Beam Program 2004*, Draft 3.0, ILC Calorimeter Test Beam Group
- [3] *The MINOS Detector Technical Design Report*, NuMI-L-603, 1 March 1999
- [4] A. Pla-Dalmau, A. Bross, V. Rykalin, "Extruding Plastic Scintillator at Fermilab" FERMILAB-Conf-03-318-E, 2003
- [5] Kuraray America Inc., 200 Park Ave, NY 10166, USA
- [6] Eljen Technology, PO Box 870, 300 Crane Street, Sweetwater, TX 79556, USA
- [7] Hamamatsu Corporation, 360 Foothill Road, PO Box 6910, Bridgewater, NJ 08807-0919, USA
- [8] 3M 8902 2" Tape from Shorr Packing Corp., 800 North Commerce Street, Aurora, Ill 60504
- [9] G. Apollinari, P. De Barbaro, M. Mishina, "CDF End Plug Calorimeter Upgrade Project", FERMILAB-Conf-94-030-E, 1994
- [10] A Dyshkant, D Beznosko, G Blazey, D Chakraborty, K Francis, D Kubik et al., "Small scintillating cells as the active elements in a digital hadron calorimeter for the e+e- linear collider detector" 2004 J. Phys. G: Nucl. Part. Phys. 30 N1-N16
- [11] Wigmans Richard 2000 Calorimetry Energy Measurement in Particle Physics (Oxford Science Publication) pp 219-220
- [12] CMS 1997 *The Hadron Calorimeter Project Technical Design Report* CERN/LHCC 97CMS TDR 2
- [13] Keithley Instruments, Inc., 28775 Aurora Road, Cleveland, OH 44139, USA
- [14] Du Pont Co. E.I. Du Pont de Nemours & Co., Fibers Department, Chestnut Run Plaza, PO Box 705, Wilmington, DE 19880-0705
- [15] D. Beznosko, A. Bross, A. Dyshkant, A. Pla-Dalmau V. Rykalin, "FNAL-NICADD Extruded Scintillator", FERMILAB-CONF-04-216-E, September 15, 04
- [16] Hitachi America, Ltd. 2000 Sierra Point Pkwy. Brisbane, CA 94005, USA